Aalborg Universitet

AALBORG UNIVERSITY
DENMARK

Distributed Dynamic Channel Allocation in 6G in-X Subnetworks for Industrial Automation

Adeogun, Ramoni; Berardinelli, Gilberto; Rodriguez, Ignacio; E. Mogensen, Preben

Distributed Dynamic Channel Allocation in 6G in-X Subnetworks for Industrial Automation

Ramoni Adeogun[(1)], Gilberto Berardinelli[(1)] Ignacio Rodriguez[(1)], Preben Mogensen[(1,2)],

[(1)] *Department of Electronic Systems, Aalborg University, Denmark*

[(2)] *Nokia Bell Labs, Aalborg, Denmark*

E-mail:{ra, gb, irl, pm}@es.aau.dk

Abstract—In this paper, we investigate dynamic channel selection in short-range Wireless Isochronous Real Time (WIRT) in-X subnetworks aimed at supporting fast closed-loop control with super-short communication cycle (below 0.1 ms) and extreme reliability (>99.999999%). We consider fully distributed approaches in which each subnetwork selects a channel group for transmission in order to guarantee the requirements based solely on its local sensing measurements without the possibility for exchange of information between subnetworks. We present three fully distributed schemes: ϵ-greedy channel allocation, minimum SINR guarantee (minSINR) and Nearest Neighbor Conflict Avoidance (NNCA) based on measurements of the minimum SINR and interference power. We further apply a centralized graph coloring scheme as a baseline for evaluating performance of the proposed distributed algorithms. Performance evaluation considering subnetwork mobility and spatio-temporal correlated channel models shows that the dynamic allocation schemes results in significant performance improvement and a reduction in the bandwidth required for supporting such extreme connectivity by up to a factor larger than 2 relative to static channel assignment.

I. Introduction

Wireless communication is identified as a major driver of the Industry 4.0 vision [1]. Due to the inherent flexibility, manageability and relatively low-cost, industrial wireless networks are expected to replace the bulky wired infrastructure of traditional industrial networks such as Ethercat [2], Profinet [3] or the time sensitive network solutions [4]. In some cases, the nature of industrial control traffic lead to requirements in terms of reliability, latency and even data rate that are beyond what can be achieved with current technologies. For example industrial closed-loop control at the sensor-actuator level may feature sub-milliseconds communication latencies [5] with extremely high reliability in order to preserve stability of the control loop.

Such tight communication requirements may also appear in other emerging applications such as brake and ignition control in intra-vehicle communication, fast closed loop control in intra-body networks and intra-avionics communication [6], [7]. Clearly these examples represent mission-critical use cases necessitating the need to guarantee extreme communication requirements (e.g., probability of outage $\leq 10^{-6}$ and latency below 0.1 ms) regardless of the experienced channel conditions. In a recent paper on 6th Generation (6G) networks [8],

autonomous subnetworks (i.e., short range independent cells comprising of a controller acting as the access point for multiple devices) are identified as potential solutions for supporting extreme connectivity with wire-like reliability (in the order of ≥ 99.999999). According to the authors, these subnetworks are expected to offload the most critical applications requiring high reliability and determinism in both spatial and temporal dimensions from existing cellular network, thereby ensuring that these applications are not disrupted in the event of poor or no connectivity from the cellular infrastructure.

An example of such subnetworks has recently been introduced in [6], [7], [9]. In [6], the authors presented visions for Wireless Isochronous Real Time (WIRT) in-X[1] subnetworks. In [9], a comprehensive discussion on an initial design covering frame structure and medium access control (MAC) for 6G in-X subnetworks is presented. This work also includes a semi-analytical evaluation of the performance and resource requirements for WIRT in-X subnetworks in dense static scenarios based on fixed channel assignments.

Despite the idealistic assumptions and lack of mobility in the analysis in [9], the results still show that multi-GHz bandwidth is required in order to support such extreme reliability and latency targets everywhere. The amount of bandwidth needed may even increase further in dynamic environments. For instance, the temporal dynamics of the propagation channel may result in large power fluctuations thereby impacting the possibility for support of successful communication loops. It should however be noted that the analysis in [9] relies on fixed channel assignment which is known to exhibit inferior performance relative to dynamic channel allocation (DCA). It is therefore expected that the resource requirements can further be reduced via dynamic allocation of the available resources.

In this paper, we investigate distributed DCA for wireless communication systems with extreme requirements. Dynamic allocation of radio resources have been extensively studied for other wireless systems albeit with more relaxed requirements (see e.g., [10]–[14]) due to its ability to adapt resource utilization based on experienced channel and/or interference conditions and to also reduce interference in the network. Most of the existing methods are either based on complex

---

[1]The acronym in-X for inside everything was introduced in [9] to highlight the multitude of emerging scenarios including in robots, in vehicles, in aircrafts, and in human bodies where these subnetworks are expected to be installed.
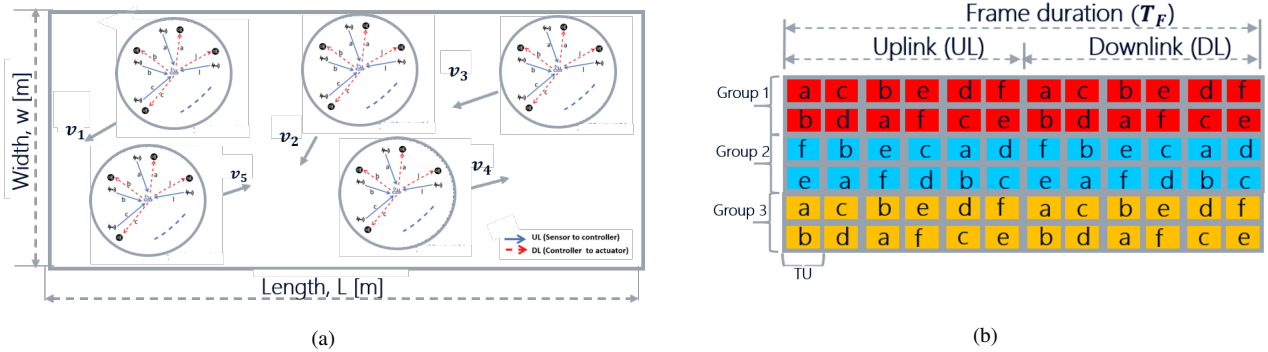
Fig. 1: Illustration of (a) a deployment comprising of 5 moving subnetworks each having a controller and multiple sensor-actuator pairs and (b) partitioning of 6 channels into 3 groups with 2 channels per group. In (b), each device is allocated two time units allowing a maximum of 2 UL and DL repetitions denoted by a,b,c,.... .

optimization algorithms (such as game theory and genetic algorithm) or require exchange of information among co-existing cells making their application to scenarios with fully independent cells and tight transmission latency unfeasible. We propose schemes based on measurements of the Signal-to-Interference-plus-Noise Ratio (SINR) on occupied channels and interference power on all channels. In these methods, the channel selection decision is performed independently by each subnetwork using local real-time sensing data obtained by the associated controller and devices. The goal of the DCA algorithms is therefore to select a channel such that the required performance limits are achieved for all devices. In summary, the main contributions of this paper are as follows:

- We investigate the potential benefits of distributed dynamic channel allocation (DDCA) in 6G in-X mobile industrial subnetworks for fast closed-loop control at sensor-actuator level.
- We present three algorithms viz: ϵ-greedy channel selection, minimum SINR guarantee (minSINR) and Nearest Neighbour Conflict Avoidance (NNCA) dynamically updating channel at each subnetwork based on experienced SINR and measured interference power.
- As a baseline for evaluating the distributed algorithms, we present a procedure for creating interference graphs based on the network topology. We further evaluate centralized channel allocation via application of greedy graph coloring to the interference graph.
- We perform simulations in a scenario with mobile in-X subnetworks and spatio-temporal correlated fading with parameters specified based on measurements from realistic industrial scenarios. The simulations indicate great potential for performance improvement and reduction in the bandwidth requirement for in-X subnetworks.

We remark here that although the DCA schemes described in this paper are presented in the context of WIRT in-X subnetworks, the algorithms can indeed be applied to any wireless system with independent cells and tight communication requirements. The remaining part of this paper is organized as follows. In section II, we introduce the WIRT in-X subnetworks and enabling technologies. We then present a description of the DCA schemes in section III followed by a

discussion of the simulation settings and results in section IV. Finally, conclusions are drawn in section V.

II. WIRT IN-X SUBNETWORKS

Consider a network with a set of $\mathcal{N} = \{1, \cdots, N\}$ independent and asynchronous mobile WIRT in-X subnetworks (WinXSs) each having M sensor-actuator pairs and a single controller as illustrated in Fig. 1a. Each controller continuously receive measurements from the sensors and then generate appropriate command to the actuators. We will henceforth refer to the sensor-to-controller and controller-to-actuator communication as uplink (UL) and downlink (DL), respectively. A combination of UL and the associated DL will be referred to as a loop. Each subnetwork (i.e, controller and devices) moves at a specified speed as shown in Fig. 1a. This can for example represents subnetworks installed in mobile robots or inside moving vehicles. As stated in [6], [7], [9], these subnetworks are required to guarantee extreme requirements: outage probability below 10^{-6} and latencies below 0.1 ms at every location. In [9], a MAC design relying on a Time Division Duplexing (TDD) frame structure with total duration, $T_F \leq 0.1$ ms as illustrated in Fig. 1b is proposed for supporting WIRT loops. The total bandwidth, B is partitioned into N_{ch} equal channels. The frame structure comprises of a DL and a UL subframe each of which is divided into N_{tu} time units (TUs). Each TU corresponds to the continuous transmission time by a device over a given channel. The main technology enablers for WinXS include:

- Periodic transmission of a fixed payload mapped at each TU over the entire channel bandwidth.
- Improved reliability via blind repetitions of a maximum of N_{rep} robustly coded packets over multiple frequency channels.
- High frequency diversity via hopping over multiple frequency channels.
- Orthogonal hopping pattern within each subnetwork and hence, no intra-subnetwork interference.

III. DYNAMIC CHANNEL ALLOCATION ALGORITHMS

Consider a network with N WinXSs and N_{ch} frequency channels over a total bandwidth, B. In [9], each subnetwork

is allowed to pre-allocate resources to devices over all channels following a random hopping pattern with a maximum of N_{rep} repetitions per device. This assignment in which each subnetwork is allowed usage of the entire bandwidth will henceforth be referred to as *no grouping*. Note that the pre-allocation is done without recourse to the experienced interference and/or channel conditions within the subnetworks. The goal of DCA is to continuously adapt the channel allocation and hopping pattern based on measurements within each subnetwork. This can, for example, be done by monitoring the interference condition at each device and switching to other channels when needed. Each device can then initiate switching decision and broadcast same to the controller and other devices resulting in huge signaling overhead and delay. Moreover, with no grouping, each device needs to choose N_{rep} out of the N_{ch} channels. This may easily become an intractable combinatorial problem in cases with large N_{ch}.

To overcome these limitations, we instead partition the N_{ch} frequency channels into K groups with equal number of channels per group, $N_{\text{cg}} = N_{\text{ch}}/K$ as illustrated in Fig. 1b and restrict transmission within each subnetwork to a single channel group at any given time. We now present the proposed DCA algorithms for dynamically switching between channel groups in order to guarantee the service requirements. The schemes which are described in the sequel rely on the following assumptions:

- The controller performs sensing of the status of all available channels and continuously obtain estimates of the interference power from all subnetworks. For simplicity, we utilize the averaged interference power over all channels within each group for the purpose of channel selection decision.Since the subnetworks are not synchronized the sensed power may either be from the controller or devices. However, due to the short range, we assume that the measurements are representative of the interference footprint.

- Each controller also has knowledge of the SINR on both the DL and UL of its associated control loops. Each controller decide to either stay on a channel group or switch to another group based on the SINR values. Considering the extreme reliability in WIRT, channel switching decision (CSD) is performed based on the minimum SINR on either the UL or DL, denoted for the nth subnetwork as $SINR_{n,\text{min}}$. Note that while the UL SINR can be estimated at the controller using the signals received from the sensors, the DL SINR needs to be reported by the devices.

- We assume that the required minimum SINR to satisfy the target outage probability, $P_{\text{out},T}$ is known by each controller and denote this as $SINR_{\text{th}}$. This can be calculated for a given configuration (i.e., bandwidth, number of receive antenna and channel model).

A. Distributed channel selection schemes

In the distributed channel selection schemes, each controller relies on its local measurements at a given time to make switching decision for the next transmission. A channel switching decision is made if the minimum SINR on either UL or DL within each subnetwork falls below a set threshold. If a decision to switch channel group is made, the controller selects a new group according to rules defined for each algorithm as follows:

1) ϵ-Greedy channel selection: Each controller selects the best channel group (i.e., with lowest aggregate interference power) with probability $\epsilon(0 \leq \epsilon \leq 1)$ or randomly with probability $1 - \epsilon$. With $\epsilon = 0$, this scheme corresponds to a fully random selection approach. On the other hand, setting $\epsilon = 1$, results in a greedy algorithm in which each subnetwork selects the best channel group regardless of the impact of such decision on other neighbouring subnetworks.

2) Minimum SINR Guarantee (minSINR): Each controller attempts to select the worst channel satisfying the required SINR threshold, i.e., $SINR_{\text{th}}$ under current observed channel conditions. If no channel satisfying the limit is available, the channel with the least interference power is selected. This approach is expected to benefit the entire network via reduced interference footprint as well as reduction in the frequency of channel switching and signaling overhead.

3) Nearest Neighbour Conflict Avoidance: In the Nearest Neighbour Conflict Avoidance (NNCA), each controller selects a channel that is not currently occupied by the $K-1$ subnetworks from which the highest interference power is sensed. Unlike the ϵ-greedy and minSINR schemes which make switching decision based on aggregate interference power, this scheme relies on the assumption that each subnetwork is able to infer the channels occupied by its nearest neighbours from its local measurements. This inference can for example be done by equipping the controller in each subnetwork with the capability of listening to reference signals from neighbouring subnetworks.

B. Centralized Graph Coloring (CGC)

As mentioned above, WIRT in-X subnetworks are expected to be independent thereby making centralized resource management unfeasible. However, as a baseline for evaluating the distributed algorithms, we studied a centralized method based on graph coloring [15] for dynamically allocating channel groups to subnetworks. This approach relies on the assumption that a dedicated processing unit (PU) which continuously collect measurements from all subnetworks for channel allocation exists.

Consider an undirected graph $G = \{\mathcal{V}, \mathcal{E}\}$, where $\mathcal{V}$ and $\mathcal{E}$ are the vertex and edge sets, respectively. Coloring of such a graph refers to the assignment of labels, i.e., colors, to its vertices such that no two connected vertices are assigned the same label [15]. In most coloring algorithms, a minimum number of colors (often referred to as the chromatic number) is required for the graph to be colorable. Clearly, this may not be the case in a WIRT network where the number of subnetworks is expected to be much larger than the number of channels to be assigned. A major task in DCA based on graph coloring is therefore the mapping of the network to a conflict graph such

TABLE I: Simulation parameters.

Parameter	Value	Parameter	Value	Parameter	Value
Deployment area [m^2]	30 × 30	PL exponent, ε	2.2	Cell radius [m]	2.5
Minimum inter-subnetwork distance [m]	1.5	Shadowing standard deviation, σ_s [dB]	3	Number of channels, N_{ch}	12
Number of controllers/subnetworks, N	16	De-correlation distance, d_c [m]	4	Number of groups, N_{gr}	[3,4,6,12]
Number of devices per subnetwork, M	18	Noise figure [dB]	10	Number of repetitions, N_{rep}	[4,3,2,1]
Velocity, v [m/s]	2.0	Transmit power per channel [dBm]	-10	Number of receive antenna	2
Simulation time [s]	2000	Lowest Frequency [GHz]	6	Per channel bandwidth [MHz]	40 - 320
Snapshot duration [s]	20	Measurement update interval [ms]	5	Payload size [bytes]	50
Waveform	OFDM	Subcarrier spacing [kHz]	480	Bandwidth per fading block [MHz]	20

TABLE II: SINR threshold with $P_{\text{out}} = 10^{-6}$

BW [MHz]	40	80	120	160	200	240	280	320
SINR$_{th}$ [dB]	40.0	20.0	13.5	10.0	7.5	5.5	4.2	3.5

it is K-colorable. The centralized graph coloring (CGC) based DCA involve the following steps.

1) Conflict Graph Creation: At each time instant, a conflict graph, G_t is created by mapping the network topology to an interference graph with nodes corresponding to subnetworks and edges defined by connecting each vertex, v to $K-1$ other vertices generating the strongest interference to v.

2) Vertex coloring: Coloring of the conflict graph is performed at every update instant using a greedy coloring algorithm [16].

IV. NUMERICAL EVALUATION

We now present models for performance evaluation of the DCA schemes as well as the simulation procedure and results.

A. Simulation assumptions and model

Assuming a block fading channel with capacity achieving codes and chase combining of the multiple repetitions over N_{rx} uncorrelated receive antennas, the outage probability after all repetitions can be expressed as [9]

$$P_{\text{out}} = \prod_{v=1}^{N_{\text{rep}}} \Pr\left[\frac{1}{L} \sum_{\ell=1}^{L} \log_2\left(1 + \sum_{z=1}^{N_{\text{rx}}} \gamma_{\ell,z} \sum_{p=1}^{v} \Gamma_p \right) < R \right].$$

(1)

where L is the number of fading blocks, R is the transmission rate, Γ_p is the average SINR on the pth channel and $\gamma_{\ell,z} = |h_{\ell,z}|^2$ is the small scale power for the zth receive antenna on the ℓth fading block with $h_{\ell,z}$ denoting the small scale gain assumed to be Rayleigh distributed.

The SINR is calculated based on the large scale desired and interference power which are computed using

$$P_{\text{rx}} = P_{\text{tx}} - \left[20\log_{10}\left(\frac{4\pi f d_0}{c} \right) + 10\varepsilon\log_{10}\left(\frac{d}{d_0} \right) + X_s \right],$$

with P_{tx} denoting the transmit power, $c \sim 3 \cdot 10^8$ m/s is the speed of light, d is the distance between the transmitter and receiver, d_0 is the reference distance, ε denotes the path-loss exponent, f is the center frequency and X_s denotes the lognormal shadow fading component (in dB). The shadow fading is modelled in this paper using the correlated model based on Gaussian random fields [17], [18]. To simulate from the model, we generate a zero-mean Gaussian random process

at equally spaced points on a rectangular grid with exponential co-variance function. Based on the generated shadowing map, the loss on a link from **a** to **b** is computed using [17]

$$X_{\mathbf{ab}} = \frac{1 - e^{(-\frac{d_{\mathbf{ab}}}{d_c})}}{\sqrt{2}\sqrt{1 + e^{(-\frac{d_{\mathbf{ab}}}{d_c})}}}(s(\mathbf{a}) + s(\mathbf{b})),$$

(2)

where $d_{\mathbf{ab}}$ and d_c denote the distance between **a** and **b** and the decorrelation distance, respectively. The terms $s(\mathbf{a})$ and $s(\mathbf{b})$ are values of the shadowing field at the associated locations.

B. Simulation settings

We now evaluate the performance of the algorithms described above via a similar snapshot based procedure to that in [9] with the parameters in Table I. The path-loss and shadow fading parameter are set based on a recent channel measurements in typical industrial environments [19]. The snapshot based simulation considers a mobility model which commences with uniform distribution of the subnetworks within a rectangular deployment area at each snapshot. Each subnetwork then move with a constant speed, v, in a random direction which is changed when the it reaches any of the four edges or it's within a distance that is less than or equal to the specified minimum inter-subnetwork distance of 1.5 m from any other subnetwork. The latter is introduced to avoid unrealistic collision of subnetworks in the simulation. At each snapshot, a shadowing map is generated. This map is used for calculating link shadow fading over a snapshot duration of about 20 s according to (2) after which a new random map is generated for the next snapshot. To be consistent with [9], we consider 8 configurations with evenly spaced bandwidth per channel between 40 MHz and 320 MHz. A subcarrier spacing and bandwidth per fading block of 480 KHz and 20 MHz, respectively, are considered.

Within each snapshot, measurements of the SINR and interference power are updated at an interval of 5 ms. Based on these measurements, each controller then compare the minimum SINR to the SINR threshold in order to make channel switching decision. The SINR threshold for switching decision is set for each bandwidth configuration as the minimum SINR at which the outage probability equal to the target of $P_{\text{out},T} = 10^{-6}$ plus a margin of 3 dB. The thresholds which are calculated for the considered configurations using (1) are shown in Table II. If a decision to switch channel group is made, the controller then apply the DCA methods described in Section III to select the channel group for the next transmission interval. To avoid potential *ping-pong* effects
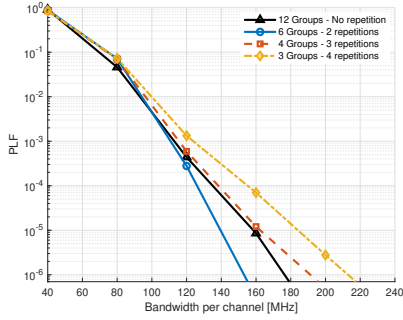
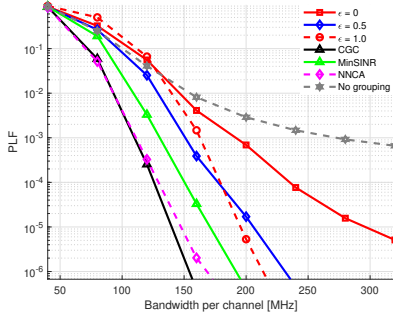Fig. 2: PLF with different number of channel groups and repetitions.

Fig. 4: Estimated total bandwidth required to achieve 10^{-4} and 10^{-6} PLF.

Fig. 3: PLF versus bandwidth per channel with different channel allocation methods.

Fig. 5: CSF versus bandwidth per channel for different dynamic channel allocation methods.

resulting from multiple subnetworks simultaneously jumping to the same group, we introduce a random switching delay. This delay is generated at the beginning of each snapshot as a random integer factor of the update interval with a maximum value of 20 ms. Thus, each subnetwork has a waiting time between 5 ms and 20 ms from selection to actual usage of the selected channel group. For the CGC, the conflict graph and color assignment are updated every 5 ms.

C. Performance results and discussion

The DDCA algorithms are evaluated using a measure of the overall service availability, i.e., the Probability of Loop Failure (PLF) defined as the probability that either or both the UL and DL associated to a control loop will fail to achieve the target outage probability, $P_{\text{out,T}} = 10^{-6}$ within the latency limit at any given time and/or location. The PLF is estimated as [9],

$$\text{PLF} = \frac{|\mathcal{S}_{\text{UL}} \cup \mathcal{S}_{\text{DL}}|}{N_{\text{total}}}, \tag{3}$$

where $|\cdot|$ denotes the cardinality of the associated set, $\mathcal{S}_{\text{UL}}$ and $\mathcal{S}_{\text{DL}}$ denote the sets of UL and DL transmissions with $P_{\text{out}} > P_{\text{out,T}}$, respectively, $\cup$ is the union operator, and N_{total} is the total number of loops over all snapshots.

The DCA schemes require additional resources for accommodating switching delay and signalling of channel selection decisions. In order to achieve reasonable resource utilization efficiency, it is necessary to minimize this overhead. Thus, algorithms with high performance and relatively low channel switching rate are more attractive. As a measure of the channel switching overhead incurred by the DCA schemes, we utilize
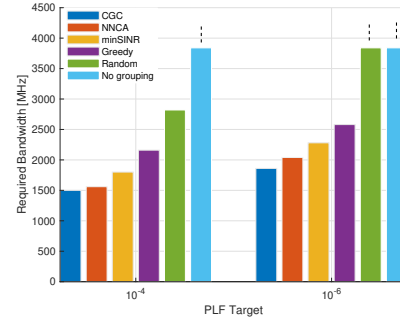
the Channel Switching Frequency (CSF) calculated as the percentage of time instants where each subnetwork performs channel switching to the total simulated time instants. The CSF is averaged over all subnetwork and snapshots. Based on the parameters in Table I, the PLF and CSF are calculated using approximately 1.152×10^8 samples translating to a statistical confidence level of 95% within a ± 18.3 % interval at the PLF target of 10^{-6}.

In order to determine the trade-off between channel group size (i.e., number of channels per group) and number of groups, we evaluate the baseline algorithm, i.e., CGC with different number of groups. For each grouping, the number of repetitions per device is set equal to the group size. Fig. 2 shows the PLF obtained using the CGC with 3(4), 4(3), 6(2) and 12(1) channel groups(repetitions). The number of repetitions (i.e, $N_{\text{rep}} = N_{\text{ch}}/K$) is a consequence of the partitioning of the total bandwidth with 12 channels. As can be seen in Fig. 2, increasing the number of groups from 3 to 6 results in improved PLF particularly at the lower percentile (below 10^{-3}). However, a further increase in number of groups from 6 to 12 results in much worse performance indicating the benefits of multiple repetitions over relative decrease in channel loading for extreme reliability. We now presents results comparing the DCA schemes with the best configuration in Fig. 2, i.e., 6 channel groups and 2 repetitions per device. We also evaluate the static channel assignment with random hopping pattern (i.e,. no grouping) and 3 repetitions per device.

Fig. 3 shows the PLF versus bandwidth per channel with all DCA schemes. The figure shows significant reduction in

PLF with DDCA algorithms relative to the static assignment without grouping and the fully random scheme translating to reduction in the bandwidth required for supporting the below 10^{-6} outage probability target up to a desired PLF within a maximum communication latency of 0.1 ms. As, expected, the CGC shows better performance than the distributed approaches. The NNCA scheme which assumes perfect inference of channels occupied by $K-1$ nearest neighbours has similar performance to the CGC except at the very low percentile. Among all methods relying on aggregate interference power measurements, the minimum SINR guarantee scheme shows the best performance. A plausible explanation for this is that in contrast to the greedy approaches, this method minimizes generated interference by only selecting the worst channel satisfying the specified SINR requirement. As shown in Fig. 3, NNCA exhibits similar performance to the centralized coloring baseline indicating the potential for optimal distributed DCA. Note that the simulation assumes perfect inference of channels occupied by each subnetwork's nearest neighbours. Some deviations are therefore expected depending on the accuracy of nearest neighbours identification procedure. Evaluation of the effect of imperfect sensing on performance and the development of protocols for practical implementation of the DCA schemes is the focus of our ongoing research.

Fig. 4 shows estimates of the total bandwidth required to support < 0.1 ms latency and $\leq 10^{-6}$ outage probability with PLF of 10^{-4} and 10^{-6}. Clearly, the DCA schemes result in significant increase in the spectral efficiency. For example, with a PLF target of 10^{-6}, the CGC, NNCA and minSINR methods require a total bandwidth of 1.8 GHz, 2.0 GHz and 2.3 GHz, respectively. Compared to the no grouping and random (ϵ-greedy with $\epsilon = 0$) schemes which require bandwidth > 3.8 GHz, these represent a factor of approximately 2.11, 1.9, and 1.65 improvement in spectral efficiency by the CGC, NNCA and minSINR, respectively. The figure also shows that while relaxing the PLF from 10^{-6} to 10^{-4} has little or no effect on the required bandwidth with static channel assignment, the DCA schemes yield a reduction of approximately 500 MHz.

The CSF results in Fig. 5 show the switching overhead incurred from each algorithm for all bandwidth configurations. The CGC scheme has equal overhead regardless of the bandwidth configuration. This is expected since the CGC is performed at every update interval without recourse to the required SINR for each configuration. The ϵ-greedy schemes has higher overhead compared to the best performing distributed scheme, i.e, NNCA. The overhead is however negligible for all schemes for the configurations with larger bandwidth. This indicates that with efficient nearest neighbour identification protocol, resource requirement for WIRT in-X subnetworks can be significantly reduced at relatively low switching cost.

V. CONCLUSION

We have presented algorithms for distributed dynamic channel allocation in 6G in-X subnetworks for applications with extreme latency and reliability requirements such as fast-closed loop control in industrial automation, brake and ignition control in vehicles and intra-avionics communications. The algorithms are simple and rely only on local sensing measurements of the SINR and interference power obtained within each subnetwork. The evaluation results in a dynamic environment with subnetwork mobility have shown great potential for improved performance with a factor larger than 2 gain in spectral efficiency. Simulation results have shown that similar performance to the centralized baseline can be achieved with the NNCA approach provided accurate identification of the nearest neighbours' channel is possible. Our ongoing research is developing protocols for enabling DDCA with the proposed algorithms and also evaluating potential for prediction-aided dynamic channel allocation.

REFERENCES

[1] B. Chen, J. Wan, L. Shu, P. Li, M. Mukherjee, and B. Yin, "Smart Factory of Industry 4.0: Key Technologies, Application Case, and Challenges," *IEEE Access*, vol. 6, pp. 6505–6519, 2018.

[2] D. Jansen and H. Buttner, "Real-time Ethernet: the EtherCAT solution," *Computing and Control Engineering*, vol. 15, no. 1, pp. 16–21, 2004.

[3] B. Galloway and G. P. Hancke, "Introduction to Industrial Control Networks," *IEEE Commun. Surv. Tutor.*, vol. 15, pp. 860–880, 2013.

[4] L. L. Bello and W. Steiner, "A perspective on IEEE time-sensitive networking for industrial communication and automation systems," *Proc. IEEE*, vol. 107, no. 6, pp. 1094–1120, 2019.

[5] A. Nasrallah, A. S. Thyagaturu, Z. Alharbi, C. Wang, X. Shao, M. Reisslein, and H. ElBakoury, "Ultra-low latency (ULL) networks: The IEEE TSN and IETF DetNet standards and related 5G ULL research," *IEEE Commun. Surv. Tutor.*, vol. 21, no. 1, pp. 88–145, 2018.

[6] G. Berardinelli, N. H. Mahmood, I. Rodriguez, and P. Mogensen, "Beyond 5G wireless IRT for Industry 4.0: Design principles and spectrum aspects," in *IEEE Globecom Workshops*, 2018, pp. 1–6.

[7] G. Berardinelli, P. E. Mogensen, and R. O. Adeogun, "6G subnetworks for life-critical communication," in *6G Wireless Summit*. IEEE, 2020.

[8] H. Viswanathan and P. E. Mogensen, "Communications in the 6G Era," *IEEE Access*, vol. 8, pp. 57 063–57 074, 2020.

[9] R. Adeogun, G. Berardinelli, P. E. Mogensen, I. Rodriguez, and M. Razzaghpour, "Towards 6G in-X subnetworks with sub-millisecond communication cycles and extreme reliability," *IEEE Access*, 2020.

[10] R. O. Adeogun, "A novel game theoretic method for efficient downlink resource allocation in dual band 5G heterogeneous network," *Wireless Personal Communications*, vol. 101, no. 1, pp. 119–141, Jul 2018.

[11] Jianping Jiang, Ten-Hwang Lai, and N. Soundarajan, "On distributed dynamic channel allocation in mobile cellular networks," *IEEE Trans. on Parallel and Distributed Systems*, vol. 13, no. 10, pp. 1024–1037, 2002.

[12] E. Kudoh and F. Adachi, "Distributed dynamic channel assignment for a multi-hop virtual cellular system," in *IEEE VTC Spring*, vol. 4, 2004, pp. 2286–2290 Vol.4.

[13] A. Adouane, L. Rodier, K. Khawam, J. Cohen, and S. Tohme, "Game theoretic framework for inter-cell interference coordination," in *IEEE Wirel. Commun. & Netw. Conf. (WCNC)*, 2014, pp. 57–62.

[14] R. O. Adeogun, "Joint resource allocation for dual band heterogeneous wireless network," in *IEEE WCNC*, 2018, pp. 1–5.

[15] J. Xue, *Graph Coloring*. Boston, MA: Springer US, 2009, pp. 1444–1448.

[16] L. Ouerfelli and H. Bouziri, "Greedy algorithms for dynamic graph coloring," in *International Conference on Communications, Computing and Control Applications (CCCA)*, 2011, pp. 1–5.

[17] P. Agrawal and N. Patwari, "Correlated link shadow fading in multi-hop wireless networks," *IEEE Transactions on Wireless Communications*, vol. 8, no. 8, pp. 4024–4036, 2009.

[18] S. Lu, J. May, and R. J. Haines, "Effects of correlated shadowing modeling on performance evaluation of wireless sensor networks," in *IEEE 82nd Vehicular Technology Conference*, 2015, pp. 1–5.

[19] M. Razzaghpour, R. Adeogun, G. Berardinelli, M. Ramsmus, P. Troels, M. Preben, and S. Troels, "Short-Range UWB Wireless Channel Measurement in Industrial Environments," in *WIMOB*, 2019.